

Investigation on Sizing of Voltage Source for a Battery Energy Storage System in Microgrid with Renewable Energy Sources

Swaminathan Ganesan¹, Umashankar Subramaniam², Ajit A. Ghodke¹, Rajvikram Madurai Elavarasan³, Kannadasan Raju⁴, Sagar Mahajan Bhaskar².

¹Schneider Electric Pvt. Ltd., Bengaluru, 560067, India.

²Renewable Energy Lab, Prince Sultan University, Riyadh, Saudi Arabia

³Electrical and Automotive parts Manufacturing unit, Chennai 600123, India

⁴Department of Electrical and Electronics Engineering, Sri Venkateswara College of Engineering, Chennai 602117, India

Corresponding author: Umashankar Subramaniam (Email: shankarums@gmail.com) and Rajvikram Madurai Elavarasan (Email:rajvikram787@gmail.com)

ABSTRACT The foremost challenge in a microgrid with Distributed Energy Resources (DER) is of managing the intermittent nature of renewable energy sources. Therefore, the extent of integration of the Battery Energy Storage System (BESS) has increased recently in a microgrid due to its versatility, high energy density, and efficiency. Generally, BESS is a grid-tied system and has fast power adjustment capability. Controversially, during the stand-alone mode, it cannot operate in the absence of a local Voltage Source (VS) which acts as a voltage and frequency reference in the network. To ensure the reliable operation of a microgrid during utility grid outage or non-availability of intermittent Renewable Energy Sources (RES), it is significant to operate the BESS with the local VS to dispatch the stored energy. This paper discusses the analytical methodology that can be adopted for identifying the most suitable rating of the VS which can act as a voltage and frequency reference for the BESS using Matlab/ Simulink. Further, a simulation was carried out against various load characteristics and it is observed that an Uninterruptible Power Supply (UPS) with a kVA capacity of 35-45% of that of the BESS with an overload capacity of 150-200% can be chosen as a feasible choice to act as the VS.

INDEX TERMS Battery energy storage system (BESS), Distributed Energy Resources (DER), Grid outage, Microgrid, Renewable Energy Sources (RES), Uninterruptible Power Supply (UPS), Voltage Source (VS),

I. INTRODUCTION

Recently, the development of microgrid has attracted the utilities greatly due to its network reinforcement and high-cost aging asset replacement [1]. Also, more renewable energy sources are getting incorporated into the power grid in the form of Distributed Generation (DG) or Distributed Energy Resources (DER) due to the increasing concerns about the environment and rising prices of energy [2-4] dominated by coal and oil reserves which grasps a major stake at 66.73% [5] as per the United Nations sustainable development goals (SDG) [6] and Paris agreement commitments [7, 8]. This increasing penetration of DERs poses new issues and challenges to the power grid such as increased voltage transients, frequency variations, loss of reliability, and power quality reduction [9, 10]. Particularly, the planning and operation of the network are becoming a serious problem to ensure its reliability [3]. Integration of

large-scale Battery energy storage system (BESS) has solved these shortcomings because of its inherent advantages such as enhancement of extent of penetration of DER, increased grid flexibility, enhanced system reliability, emergence of new energy business models, and support to distribution system operators [11, 12]. Specifically, BESS coupled with power electronic converter systems offers rapid response for frequency regulation and load changes. It is considered as the most viable and promising approach [13, 14] which minimizes the active power oscillation and the settling time in smart grid power systems.

The recent advancements in Lithium-ion battery technology also offer various benefits in smart grids like high power, longer life, and high charge and discharge efficiency [15-17]. In addition to a small size and low weight, Li-ion batteries can offer high energy density and storage

efficiency [18], which makes them suitable for portable devices. It also deals with high fluctuating demands and is used to compensate for long-term and low-frequency power demands [19]. It plays a crucial role to realize the flexible mechanism and optimal operation of active distribution networks. Hence, the placement and sizing of BESS directly influence the active management capability using DERs and the economic benefits of active distribution network operation [20-22]. Further, a rule-based control method for a BESS is proposed by integrating with RES to dispatch energy on an hourly basis [23]. On other hand, the use of BESS is still an expensive option and the control and supervision strategies are mandatory for their optimal performance according to the SOC (state of charge) values and deep discharge constraints [24]. In order to maintain the distribution system economically, the sizing and placing of DGs with working constraints need to be carried out.

Comparing the benefits and shortcomings of the BESS in the grid-tied system, it is determined that the BESS cannot be operated in the absence of the main grid. Therefore, this work focuses on finding the judicious sizing of the Voltage source (VS) for the BESS based on the network characteristics. It can provide the reference parameters to the BESS during the outage of the grid and also provide the unbalanced currents to loads [25]. In order to demonstrate the proposed system, a 100kVA Li-ion battery based Battery Energy Storage System (BESS) is considered which is specifically meant for brownfield projects. It consists of three-phase four wire systems [26] and consumes three balanced currents for charging and also provides three balanced currents while discharging. Therefore, it can be modeled as a three-phase current source. This sizing methodology supports the system to continue its operation with the help of VS based BESS effectively which can act as a voltage and frequency reference during outages. The main objectives of the study are as follows;

- To design the Voltage Source-based BESS to supply both real and reactive power to the load during grid outages.
- To formulate the reference current generation procedure for the BESS.
- To derive the ramping up scheme of BESS.
- To compute the optimum sizing of the VS ratings for an effective hybrid microgrid.

The article begins with an overview of the technical and economic performance features and the current research and development of BESS technologies. Following this, modelling of the test case is performed for grid-connected and islanded mode in section II. Further, this paper presents a detailed summarization of network description and operational strategy with their corresponding technical specifications in section III. Then, section IV illustrates all the test results under different modes of operation. Finally, section V concludes the article with the key observations on the benefits and the applicability of BESS.

II. MODELLING OF THE TEST SYSTEM

The microgrid architecture of the proposed system consists of various energy sources, BESS, and loads as illustrated in Figure 1. The Photovoltaic (PV) source and BESS are connected in conjunction with the utility grid to form a power system that delivers power to different types of loads as defined. Notably, all critical loads are fed through a UPS and non-critical (shedtable) loads are fed directly [27]. The Battery Energy Storage System (BESS) is connected to a low voltage network as shown in Figure 1 and it can consume and generate the active and reactive power. Preferably, it is installed in a network where several loads and distributed energy resources are connected in its proximity. The interconnection of the BESS and the micro-sources along with various loads creates a local network that is connected to the main grid by a single point (PCC). During normal operation i.e. grid-connected mode, the main grid acts as a voltage and frequency reference i.e. VS to the entire network including the BESS. When the outage of the grid happens, UPS acts as VS and provides voltage and frequency reference to the BESS and PV inverter. The response time of a BESS is ranging from 0.5 to 1 seconds i.e. time required to ramp up completely and start feeding the loads once the grid is withdrawn [28, 29]. The complete specifications of the BESS are listed in Table I. Further, the general single line diagram of the BESS under consideration is shown in Figure 2. The battery management system (BMS) aids to sense and control the system parameters. The energy management system (EMS) optimizes the managed loads on the network using two different modes as depicted below.

A. GRID-CONNECTED MODE

The single line diagram of the network during the grid-connected mode of operation is shown in Figure 3. In order to ensure a safer switching, Circuit Breakers (CB) B1 and B2 serve as interlock breakers to guarantee that only one source acts as the VS at a time [30]. Initially, the breaker B1 is in a closed position to ensure the grid integration and B2 is in open position to provide isolation between two different categories of loads. Under these circumstances, grid supplies the power to both loads distinctly (critical and non-critical loads). During outages, the sensing circuit of B1 detects the grid status and sends a command signal to open the breaker B1 and closes the breaker B2.

B. ISLANDED NETWORK

During a blackout i.e. when no grid is available; the BESS can supply power to the network along with a local voltage source (B1 open and B2 closed). A single line diagram of such an islanded network is depicted in Figure 4. The voltage source will act as a grid forming source and provide voltage and frequency reference for the balanced currents generated by the BESS. Also, the it would act as a primary element for feeding any unbalance in the islanded network.

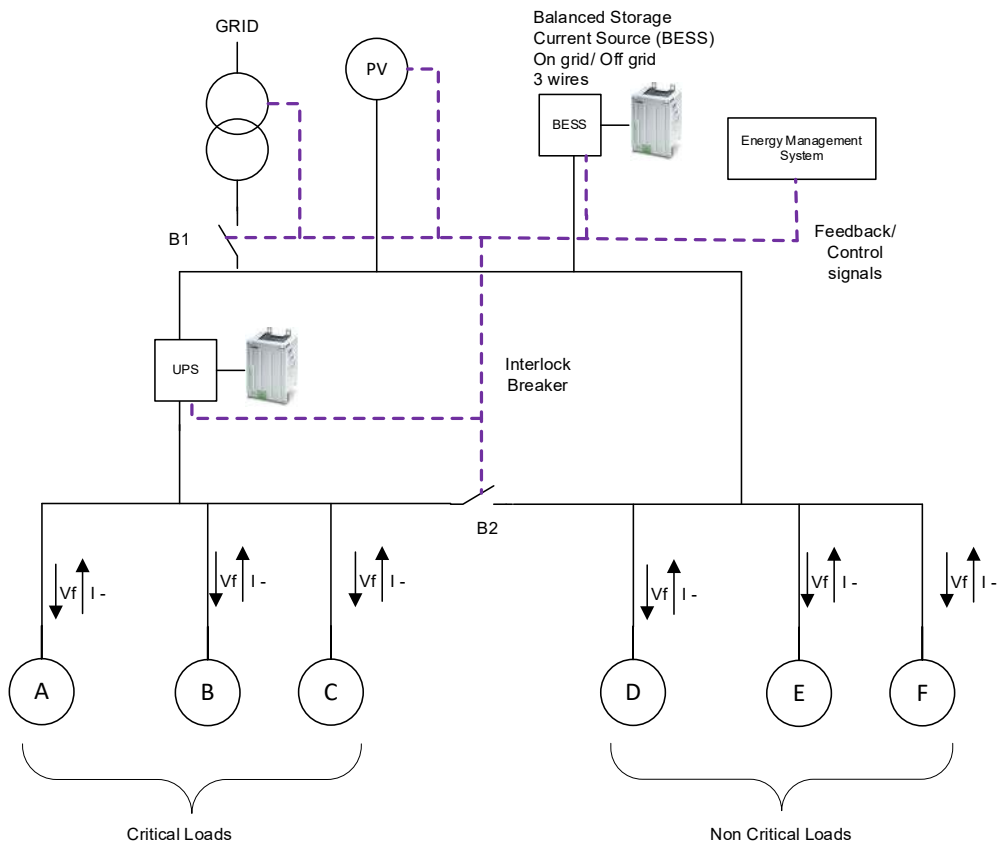


FIGURE 1. Microgrid architecture of the proposed system involving DERs, BESS and loads

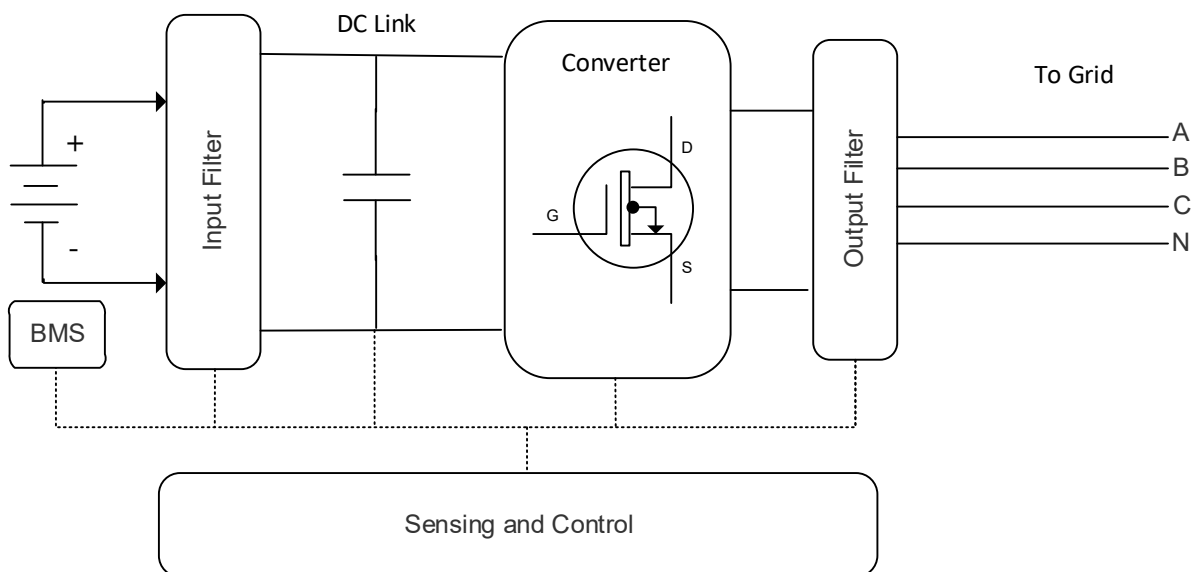


FIGURE 2. Simplified block diagram of the BESS

TABLE I
TECHNICAL SPECIFICATIONS OF BESS

S. No	Parameters	Values
1	Input Voltage	400 V
2	Input Frequency	50 Hz
3	Nominal Current	150 A
4	Current THD	<4% @ nominal Power
5	Nominal Power	150 kVA
6	Efficiency	>95%
7	Output Voltage	540 VDC to 730 VDC

TABLE II
NETWORK CONFIGURATION OF THE MICROGRID ARCHITECTURE

S. No	Type of Source/Load	Specification
1	Total Network capacity	500 kVA, 400V, 3 PH, TT grounding system
2	BESS	100 kW, 50 kWh
3	Managed Loads	400 kVA, Air conditioner, Heater, & Standard 16 A Loads
4	Priority unmanaged loads (1 PH)	Ph 1-N 230 V, Lighting: 13 kVA, PF 0.7
		Ph 2-N 230 V, Lighting: 8 kVA, PF 0.55
		Ph 3-N 230 V, Lighting: 16 kVA, PF 0.85
5	Priority unmanaged loads (3 PH)	Ph 1-N 230 V, Loads: 12 kVA, PF 0.8
		Ph 2-N 230 V, Loads: 14.3 kVA, PF 0.6
		Ph 3-N 230 V, Loads: 3.5 kVA, PF 0.67
6	Critical unmanaged loads (3 PH)	400V, 3 PH+N: 29.34 kVA, PF 0.92
		400 V, 3 PH+N: 6.45 kVA, PF 0.93

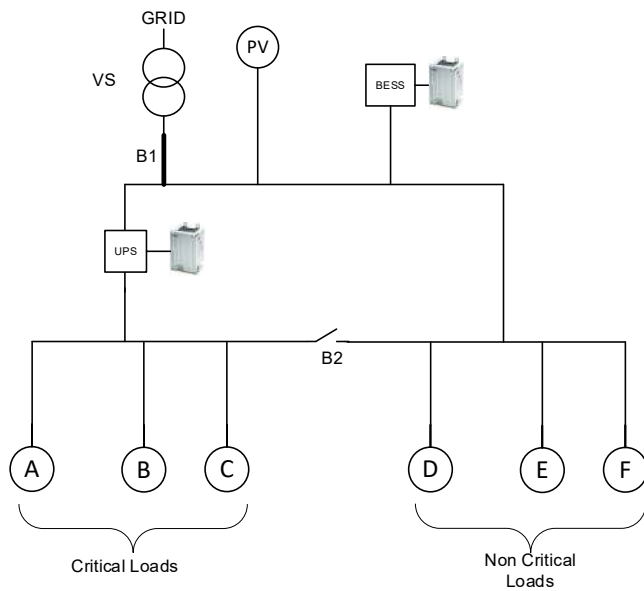


FIGURE 3. Single line diagram of the proposed microgrid involving BESS in Grid-connected mode

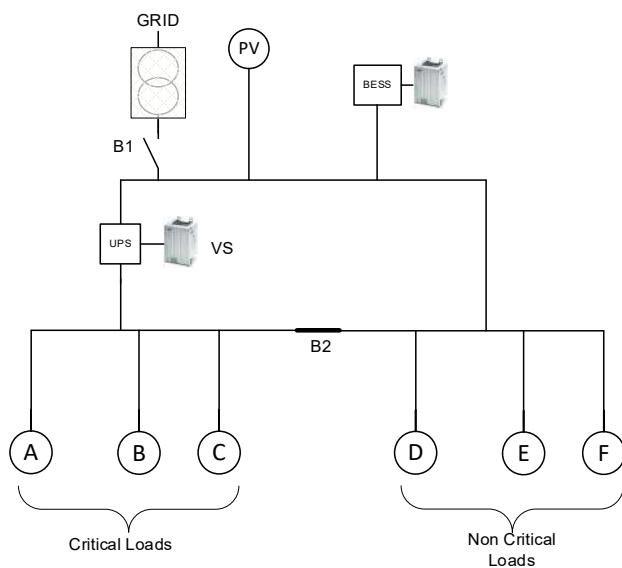


FIGURE 4. Single line diagram of the proposed microgrid involving BESS in islanded mode

III. NETWORK DESCRIPTION AND OPERATIONAL STRATEGY

The validation of the aforementioned modes of the test system is carried out with the help of a continuous simulation using the Matlab/Simulink platform. The complete specifications of the grid-connected system are illustrated in Table II. The dynamic behavior of loads such as unbalance and non-linearity is introduced in the same network in order to estimate the size of the voltage source under diverse conditions. Further, all managed or sheddable loads such as air conditioning, heater, standard 16A loads etc. are switched off during grid outage and hence they are not considered for the off-grid scenario. A separate UPS is provided to feed critical unmanaged loads during grid outage through BESS. Also, the contributions of any renewable energy sources are not considered during this situation. Therefore, the BESS takes complete responsibility for feeding the single-phase and three-phase priority unmanaged loads during the absence of the grid. Importantly, BESS takes about 0.8 to 1 seconds to ramp up the capacity to feed these loads. During this transient time interval, the voltage source has to supply the entire islanded network. After the period of 1 second, BESS ramps up completely to feed the entire active component and some reactive component of the balanced positive sequence current. The remaining part of reactive power as well as power amounting for feeding unbalance and harmonic generating loads are to be fed by the voltage source.

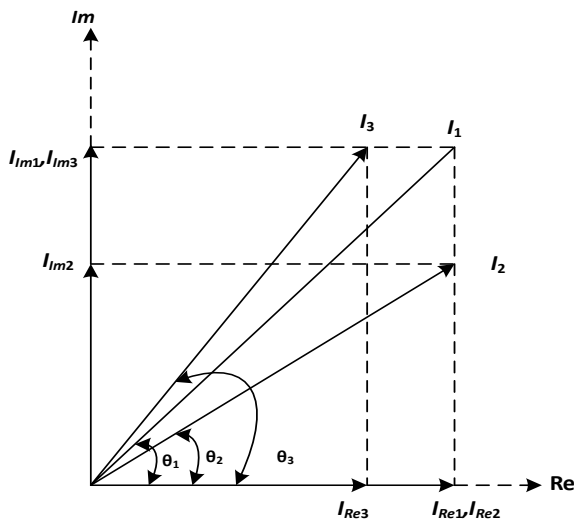


FIGURE 5. Phasor diagram representation of BESS reference current generation

The modeling of various blocks of the system and the methodology used to generate the reference currents for the BESS are explained as below. The grid is modeled as a 3-phase, 400V, 50Hz voltage source without any source impedance. As already mentioned in the earlier section, only the priority unmanaged single and three-phase loads are connected on the network. The voltage source acting as a reference forcing function for the BESS is modeled by a 3-phase, 400V, and 50Hz programmable voltage source block without any source impedance. The BESS which essentially acts as a current source is modeled by a voltage source inverter (VSI). It is assumed that the BESS batteries are already charged completely and hence the VSI is fed by a DC source which represents the battery storage block of the BESS. In order to operate the VSI as a current source, the VSI currents are controlled by hysteresis current control [31]. The reference BESS currents (to be followed by the BESS) and actual BESS currents are compared and complementary gate pulses for two switches in an inverter leg pertaining to a particular phase are generated using relay and Boolean logic blocks. The detailed phasor representation of reference current generation for BESS is shown in Figure 5.

The total load current in three-phase system is measured using three-phase VI measurements block in Simulink and fed to the three-phase sequence analyzer. It measures the magnitude and phase of the positive sequence component of the total load current [32]. From the magnitude and phase of this balanced component, both active and reactive parts are found. It is possible to make the BESS feed 100% of both active and reactive parts of the positive sequence component. Also, the BESS can feed a part of both active and reactive components as designated by the user through the desired percentage of active or reactive components. Assuming that I_1 is the magnitude of the balanced positive sequence component of the total load current obtained from the three-phase sequence analyzer block and resolving it across real

and imaginary axes as shown in Figure 5, then it can be seen that I_{Re1} and I_{Im1} are the respective active and reactive components of current I_1 .

If the BESS is made to feed both these components at 100%, then $I_1 \angle \theta_1$ will be the reference balanced current to be fed by the BESS. If the BESS is to be made to feed the total active component i.e. $I_{Re2} = I_{Re1}$ and a part of the balanced reactive component i.e. $I_{Im2} < I_{Im1}$, then the effective BESS reference current magnitude and phase is recalculated as follows,

$$|I_2| = \sqrt{I_{Re2}^2 + I_{Im2}^2} \quad (1)$$

$$\theta_2 = \sin^{-1} \left(\frac{I_{Im2}}{I_2} \right) \quad (2)$$

Likewise, if the BESS is to be made to feed the total reactive component ($I_{Im3} = I_{Im1}$) and a part of the balanced active component ($I_{Re3} < I_{Re1}$), then the effective BESS reference current magnitude and phase can be calculated respectively as follows,

$$|I_3| = \sqrt{I_{Re3}^2 + I_{Im3}^2} \quad (3)$$

$$\theta_3 = \sin^{-1} \left(\frac{I_{Im3}}{I_3} \right) \quad (4)$$

Moreover, the percentage of balanced reactive component to be fed by the BESS is restricted to 30% for the simulation study. Based on the desired percentage of active and reactive components, the resultant magnitude and phase of the effective balanced current to be fed by the BESS is obtained. Using this phase information and the simulation time (obtained using a digital clock block); three unit sinusoidal waveforms are generated using a Matlab embedded function. These three unit sinusoidal waveforms thus generated are multiplied by the magnitude of the effective balanced current to be fed by the BESS. Thus, the three-phase reference currents for the BESS are obtained. Later, the three-phase currents fed by the VSI (representing the BESS) are controlled in such a way that they follow the aforementioned three-phase reference currents which is achieved by hysteresis current regulators.

The average active and reactive powers fed by the voltage source and the BESS are measured by averaging the outputs of a three-phase instantaneous active and reactive power block. The total apparent powers fed by the voltage source and BESS are also computed in the same block. In order to have a quantitative idea about the unbalance in the network, a single value representing percentage unbalance is calculated from load currents utilizing the following formulae.

$$\overline{I_{rms}} = \frac{1}{3} \sum_{n=1}^3 I_{rms_n} \quad (5)$$

TABLE III
ACTIVE, REACTIVE AND APPARENT POWERS FED BY THE BESS AND THE VOLTAGE SOURCE

S. No.	Percentage Current unbalance	Percentage of nonlinear loads	Active, Reactive and Apparent powers supplied by the voltage source during transient period: 0.5 s to 1.4 s (no BESS)			Active, Reactive and Apparent powers supplied by the voltage source during steady-state: 1.4 s to 3.0 s (with BESS)			Active, Reactive and Apparent powers supplied by the BESS during steady-state: 1.4 s to 3.0 s			Active, Reactive and Apparent powers of the loads on the network			$\frac{kVA_{VS}}{kVA_{BESS}}$
			kW	kVAR	kVA	kW	kVAR	kVA	kW	kVAR	kVA	kW	kVAR	kVA	
1	3.41	19	78.8	53	95	0.8	36.7	36.8	78	16.3	79.8	78.8	53	95	0.461
2	4.2	9.8	77.6	56	95.7	0.8	38.8	38.9	76.9	17.2	78.8	77.6	56	95.7	0.493
3	8.9	5.3	73.2	54.8	91.4	0.8	38	38.1	72.5	16.8	74.4	73.2	54.8	91.4	0.512
4	10.62	17.47	71.2	49.9	87	0.7	34.6	34.6	70.6	15.3	72.2	71.2	49.9	87	0.479
5	11.19	17.14	85.1	61.9	105.2	0.8	42.9	43	84.4	19.1	86.5	85.1	61.9	105.2	0.497
6	13.51	5.8	60.8	47.4	77.1	0.7	32.9	32.9	60.1	14.5	61.8	60.8	47.4	77.1	0.532
7	15.03	20.67	90.2	58	107.3	0.8	40.1	40.2	89.6	17.9	91.3	90.2	58	107.3	0.440
8	17.27	5.1	67.5	54.1	86.6	0.7	37.6	37.6	66.8	16.6	68.9	67.5	54.1	86.6	0.545
9	23.15	5.824	65.9	50.1	82.8	0.8	34.8	34.9	65.3	15.4	67.1	65.9	50.2	82.9	0.520
10	30.32	19.61	58.2	33.3	67	0.7	23	23	57.5	10.3	58.4	58.2	33.3	67	0.393

$$\Delta I_{rms} = \frac{1}{3} \sum_{n=1}^3 |I_{rms} - I_{rmsn}| \quad (6)$$

$$\text{Percentage Unbalance} = \frac{\Delta I_{rms}}{I_{rms}} \times 100 \quad (7)$$

Where I_{rms} is the RMS value of the fundamental current of the 'n'th phase, I_{rms} is the average of RMS values of all the three-phase currents and ΔI_{rms} is the average of the absolute deviation of RMS value of each phase current from the average of the RMS values of all three-phase currents. The priority unmanaged single and three-phase loads indicated in Table II are further modified in order to have more unbalance in the network. Also, single-phase diode bridge rectifier loads are introduced in order to increase the penetration of nonlinear loads.

IV. RESULTS AND DISCUSSION

In order to illustrate the effectiveness of the proposed scheme, the simulation was carried out into three events based on the time interval as follows,

Event 1: From the start of execution to 0.5 seconds

In this case, the main grid is considered initially which feeds the priority unmanaged single and multi-phase loads. Subsequently, the grid is withdrawn after 0.5 seconds by opening a three-phase circuit breaker. It is noted earlier that all managed loads are not considered for the simulation study.

Event 2: (From 0.5 to 1.4 seconds)

In this case, the voltage source which is essentially in a "hot standby" mode detects the absence of the grid and connects to the network at 0.51 seconds. The BESS is allowed to ramp up to feed the network from 1.4 seconds onwards and the voltage source is responsible for feeding the entire network for approximately 0.9 seconds. During this transient time, the voltage source has to meet the entire power demand of the network amounting to (active + reactive + unbalance + harmonic) loads.

Event 3: (From 1.4 to 3.0 seconds)

During this period, The BESS starts feeding the balanced part of the active (100%) and reactive (30%) components of the total load current as designated by the user. In the course of the steady-state interval, the voltage source is responsible for feeding the remaining reactive power of the network as well as any unbalanced and harmonic currents.

The simulation is executed for all the aforementioned events/schemes and the powers fed by the voltage source and the BESS are measured. The combination of different values of unbalanced current along with different penetration of nonlinear loads is also incorporated. Table III shows the net power fed by the BESS through voltage source during all three operating events against various percentages of current unbalance and nonlinear loads. It is observed that the steady-state and transient mode kVA ratings of the voltage source are estimated to be between 35 and 50 kVA. It should possess 150-200 % of overload capabilities in order to handle the loads in a transient time interval. Additionally, it is noted that the summation of apparent powers for the BESS and the voltage source will not encompass the total apparent power

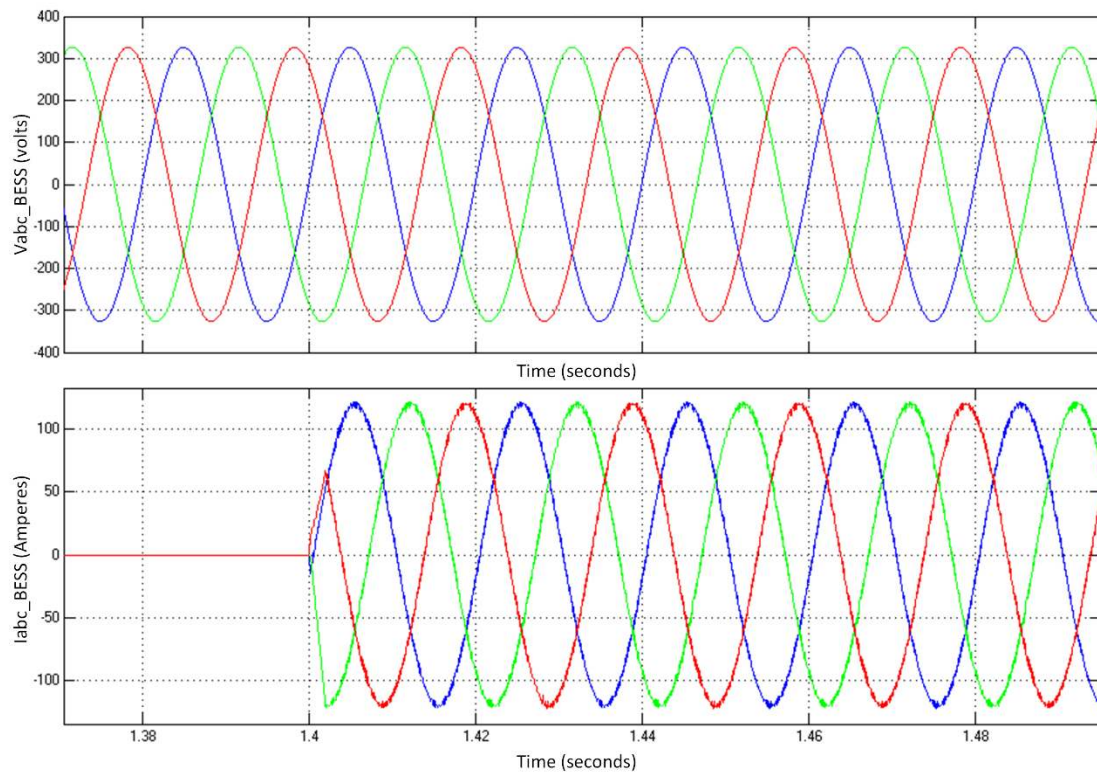


FIGURE 6. Three-phase currents fed by the BESS

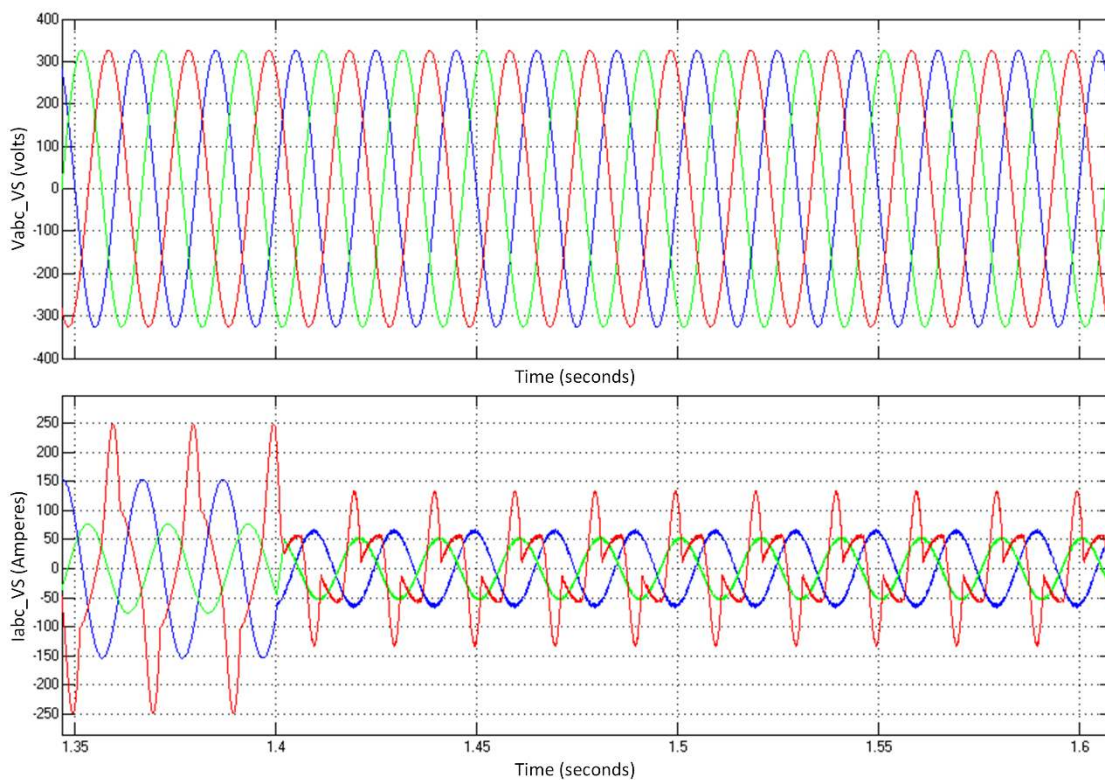


FIGURE 7. Three-phase voltages and currents fed by the voltage source

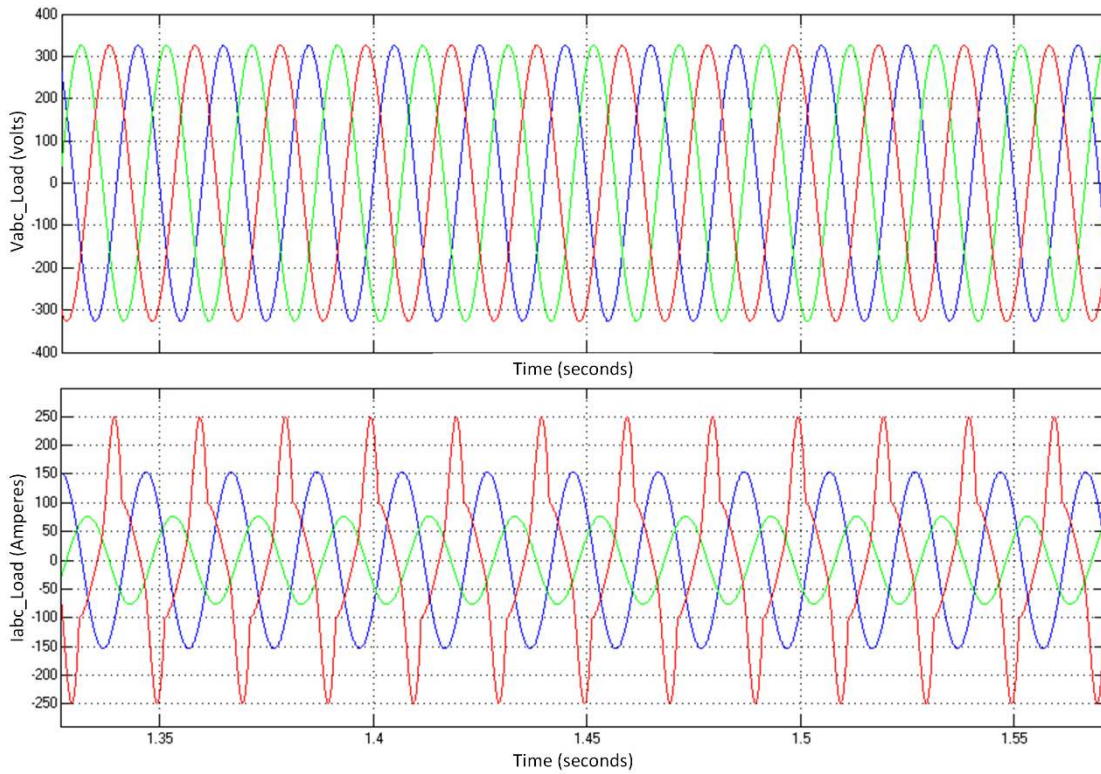


FIGURE 8. Three-phase load currents priority unmanaged loads with unbalance and nonlinear loads

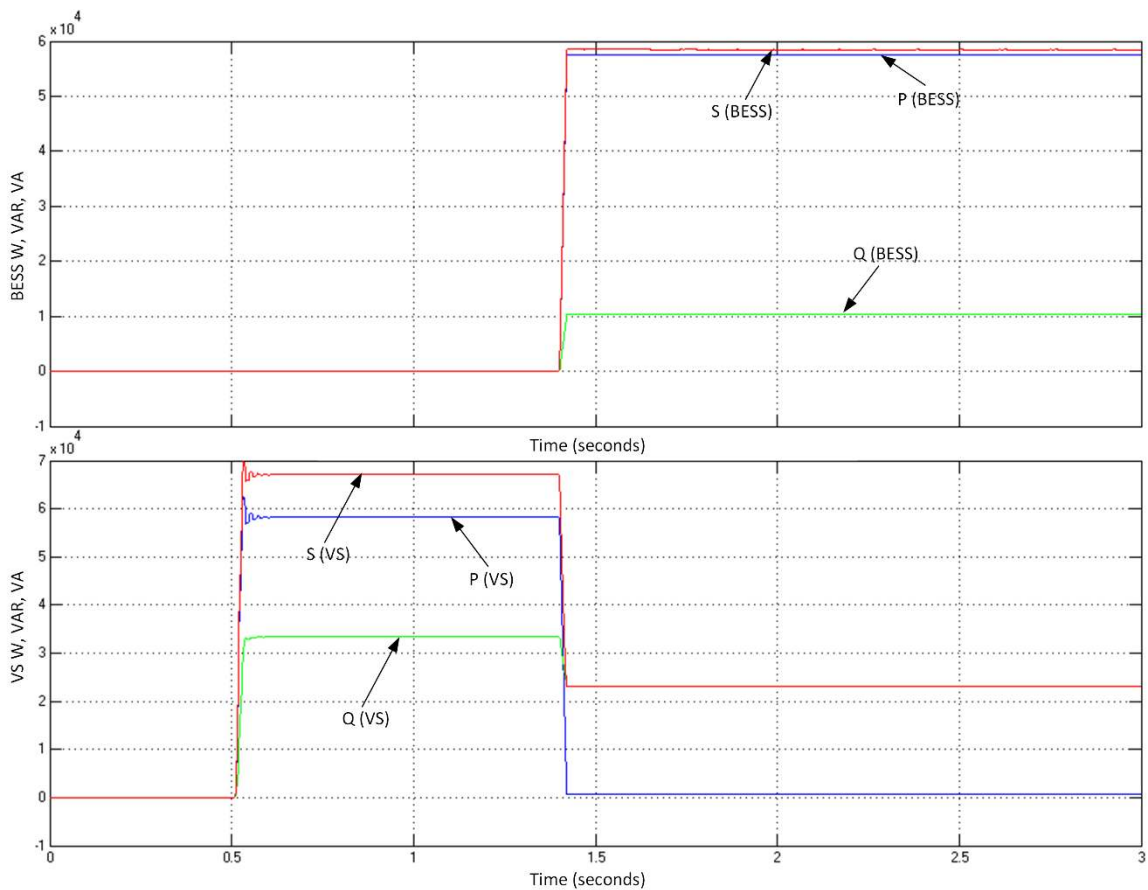


FIGURE 9. Active and reactive powers supplied by the BESS and the voltage source

accurately because they do not have the same displacement between current and voltage. Moreover, the three-phase current and voltage fed by the BESS during the transient period (i.e. before 1.4 seconds) and the steady-state (after 1.4 seconds) are shown in Figure 6. It is perceived that the BESS is supplying a uniform balanced current through all three-phases after 1.4 seconds. Furthermore, the three-phase current and voltage fed by the voltage source during the transient and steady-state periods are shown in Figure 7. It indicated that the voltage source is feeding the entire three-phase load currents (active power, reactive power, unbalance, and harmonic) during the transient period. As soon as the BESS is admitted (at 1.4 seconds), it starts supplying about 30% of the balanced reactive component. Subsequently, during the steady-state period, the voltage source supplies less current than the earlier event and it encompasses of remaining reactive component along with unbalancing and harmonic currents.

Therefore, the BESS is released from supplying any unbalance harmonic currents. Further, the total three-phase load currents for priority unmanaged single and three-phase loads with unbalance and nonlinear loads are depicted in Figure 8. It is observed that the three-phase loads continue to consume the same current during the transient and the steady-state when the BESS is operational.

It is an important task to estimate the power fed by the BESS and the voltage source during different events and the observed results from simulations are shown in Figure 9.

From the observation, it is noted that the active power fed by the voltage source during steady-state (after 1.4 s) is negligible. Hence, the kVA rating of the voltage source during steady-state is dominated by the reactive power fed by it.

Further, this work focuses on estimating the optimum VS rating for efficient hybrid system design against various parameters such as percentage variation of current unbalance, nonlinear loads, and power factors.

A. EFFECT OF CURRENT UNBALANCE

Primarily, the effect of the percentage of current unbalance on the ratio of KVA ratings is analyzed with a constant nonlinear load while the percentage of current unbalance is varied for each event. Moreover, the ratio of steady-state kVA ratings of the voltage source and BESS is calculated for each case and displayed in Table IV. It represents two cases with 10% and 20% of nonlinear load in a combination of current unbalance ranging from 6% to 35%. Notably, during the load magnitude of 73.3 kVA with 6.4% of current unbalance and 10% nonlinear load, the optimum capacity of voltage source and BESS are 27.9 kVA and 61.8 kVA respectively. Importantly, the ratio of VS rating to BESS rating is presented in the last column of the table and it helps in arriving at optimum capacity for VS. Therefore, oversizing of VS can be avoided for various depicted scenarios given below.

TABLE IV
EFFECT OF PERCENTAGE OF CURRENT UNBALANCE ON THE RATIO OF KVA RATINGS

S. No.	Percentage of nonlinear loads	Percentage current unbalance	kVA_{BESS}	kVA_{VS}	Total load KVA	$\frac{kVA_{VS}}{kVA_{BESS}}$
1	10	06.4	61.8	27.9	73.3	0.451
		09.8	57.5	25.6	68.0	0.445
		11.9	77.8	38.0	94.3	0.488
		18.5	70.7	33.6	85.1	0.475
		23.4	66.0	30.6	78.9	0.463
		28.8	63.5	29.2	75.8	0.459
2	20	04.0	72.2	30.3	84.0	0.419
		06.0	66.5	27.3	77.0	0.410
		13.5	65.2	26.5	71.7	0.406
		15.7	67.7	28.1	78.5	0.415
		21.5	74.3	31.7	86.8	0.426
		27.3	69.5	31.0	82.2	0.446
		34.1	59.4	23.6	68.2	0.397

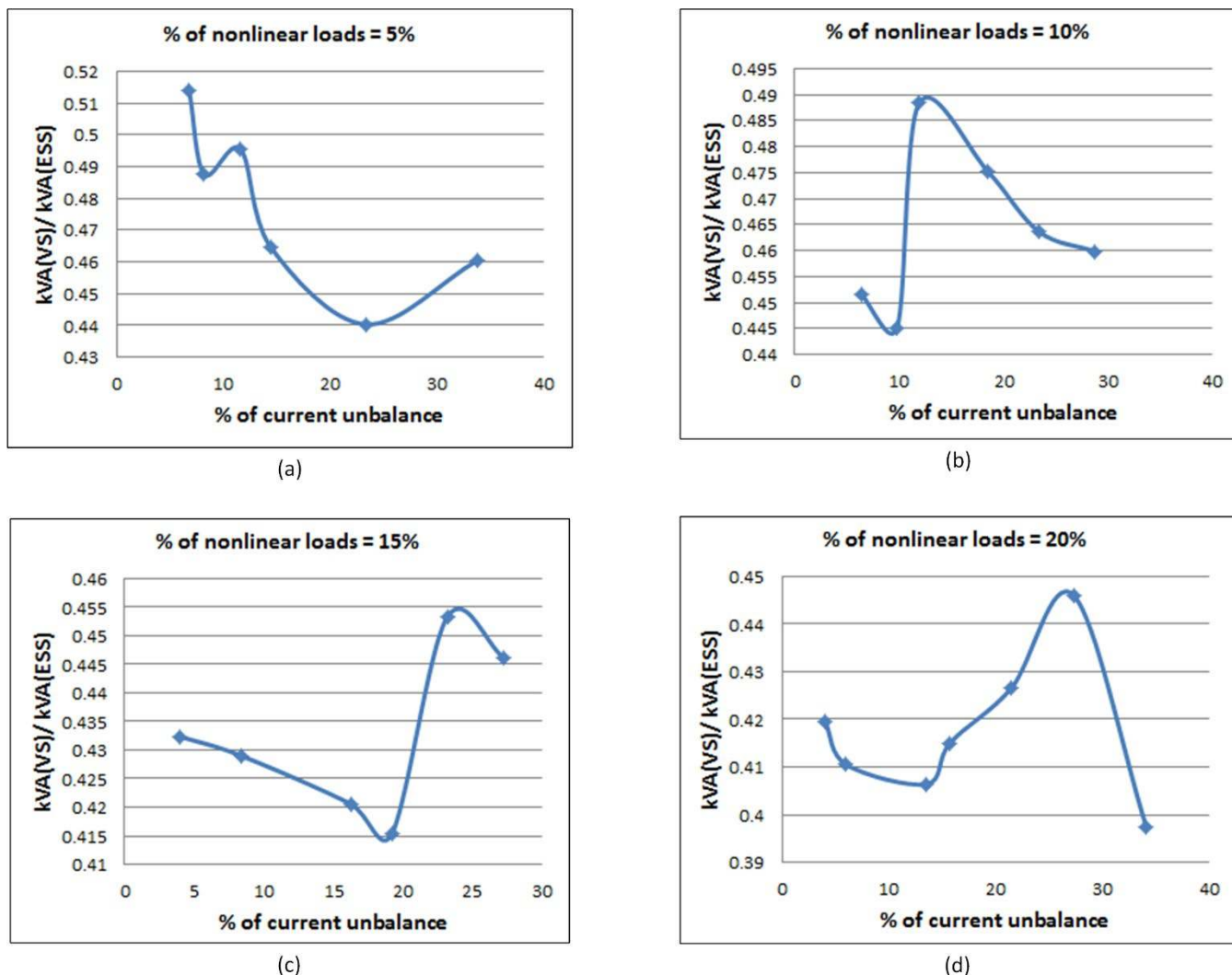


FIGURE 10. Effect of percentage of current unbalance on the ratio of kVA ratings when percentage of nonlinear loads is held constant at (a) 5%, (b) 10%, (c) 15% and (d) 20%

TABLE V
EFFECT OF PERCENTAGE OF NONLINEAR LOADS ON THE RATIO OF KVA RATINGS

S. No.	Percentage Current unbalance	Percentage of nonlinear loads	kVA_{BESS}	kVA_{VS}	Total load KVA	$\frac{kVA_{VS}}{kVA_{BESS}}$
1	5	5.000	72.7	35.5	89.0	0.488
		9.400	75.2	36.6	91.1	0.486
		15.60	76.3	34.6	90.6	0.453
		20.47	65.4	28.5	75.5	0.435
2	15	05.0	64.5	31.6	78.30	0.489
		09.5	56.6	25.3	67.00	0.446
		14.5	76	33.8	90.50	0.444
3	25	19.0	88.4	39.1	104.4	0.442
		05.6	58.0	27.2	69.5	0.468
		09.3	57.7	26.0	68.3	0.450
		14.5	55.8	23.2	65.0	0.415
		19.0	60.6	24.6	70.0	0.405

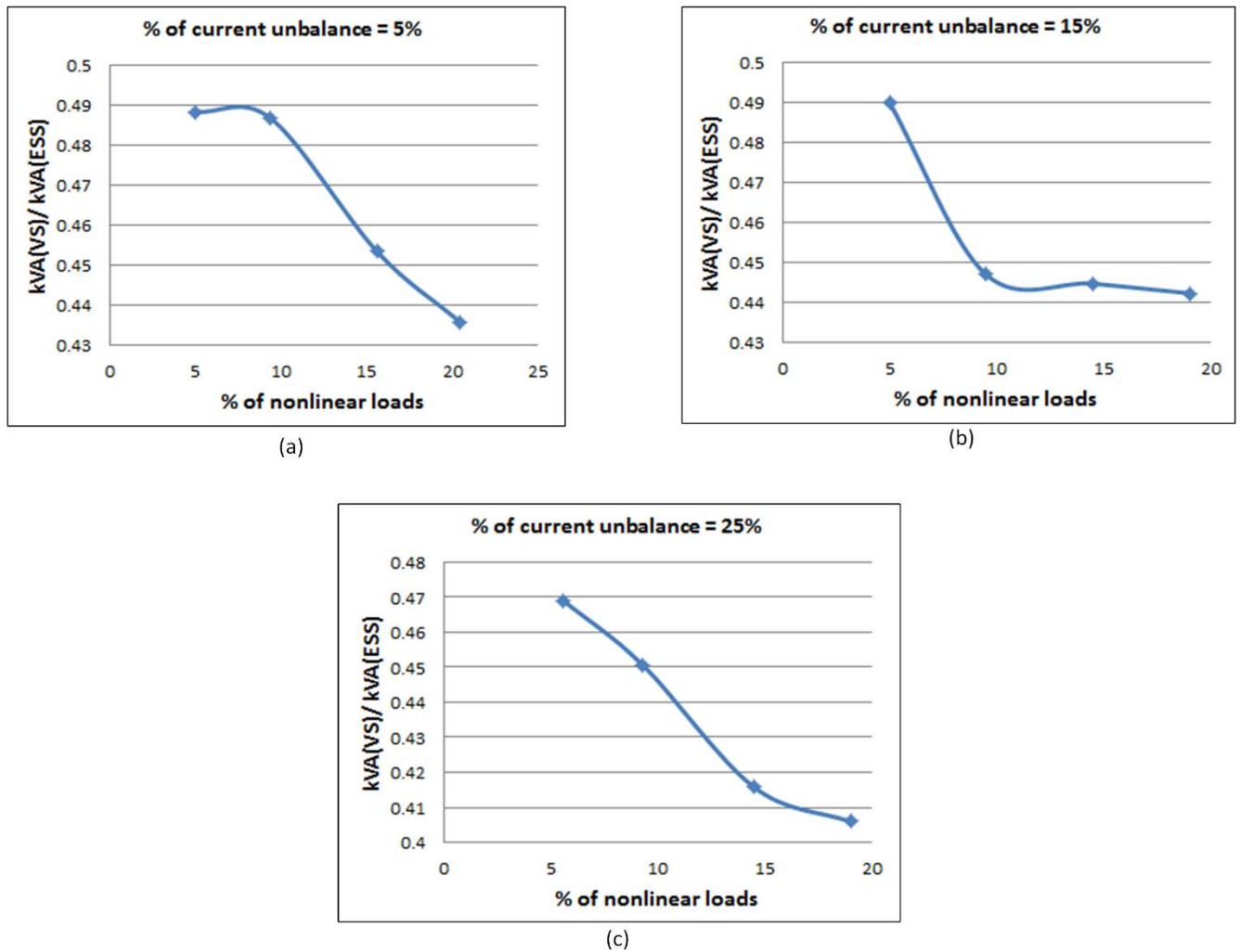


FIGURE 11. Effect of percentage of nonlinear loads on the ratio of kVA ratings when percentage of current unbalance is held constant at (a) 5%, (b) 15% and (c) 25%

TABLE VI
EFFECT OF TOTAL LOAD POWER FACTOR AND PERCENTAGE OF CURRENT UNBALANCE ON THE RATIO OF kVA RATINGS

S. No	Percentage of Nonlinear loads	Percentage of Current unbalance	kVA_{BESS}	kVA_{VS}	Total load kVA	Total load PF	$\frac{kVA_{VS}}{kVA_{BESS}}$
1	20.21	13.54	65.3	26.5	75.4	0.860	0.40
		34.60	67.6	24.9	76.4	0.880	0.37
		36.00	63.5	28.3	75.1	0.838	0.44
		31.00	64.2	31.8	78.2	0.80	0.49
		30.00	63.8	33.2	79.0	0.79	0.5204
2	10.83	19.41	63.5	25.1	72.9	0.867	0.3955
		10.89	67.6	19.3	73.2	0.923	0.29
		08.80	70.1	25.2	78.8	0.886	0.3595
3	15.00	25.22	67.0	25.7	76.4	0.873	0.3837
		07.60	61.0	24.6	70.5	0.862	0.4035
		09.20	65.4	24.8	74.4	0.875	0.3801
		20.81	66.3	21.2	73.1	0.906	0.3205

Likewise, the percentage of current unbalance is plotted against the ratio of kVA rating (KVA_{VS}/KVA_{BESS}) for each aforementioned event by keeping the load nonlinearity constant and the same is illustrated in Figure 10. It is evident that the 5% of nonlinear load along with 20% to 30% of current imbalance stretches the minimum VS rating requirement, whereas the VS rating requirement is higher for less than 10% current unbalance. Further, during 10% nonlinear loads in the network, 10% of current unbalance condition requires minimum VS rating. Likewise, 15% of nonlinear loads require a minimum VS rating with 20% of the unbalance current. Finally, with 20% nonlinear loads in the system, again the VS rating requirements become low with 35% unbalance current condition. Consolidating these inferences, it helps to choose the optimum VS rating for a given nonlinear nature of load and percentage of current unbalance.

B. EFFECT OF PERCENTAGE OF NONLINEAR LOADS

Similar to the previous case, the simulation is executed for constant current unbalance (5%, 15%, and 25%) against the varied percentage of nonlinear loads for each event and the observed results are shown in Table V. It is inferred that the ratio of KVA ratings between VS and BESS is arrived to find out the optimum VS rating requirement for a specific load condition with different load nonlinearity and current unbalance. Particularly, during 5% current unbalance and 5% nonlinearity in a total of 89 kVA load, the minimum VS and BESS rating are estimated to be 35.5 kVA and 72.7 kVA respectively. Figure 11 shows curves plotted for different load current unbalance percentages for varying percentage of nonlinear loads to identify the optimum VS to BESS kVA rating. During the load, current unbalance of 5%, 15%, and 25%, the percentage variation of the nonlinear loads requires a reduced KVA ratio.

C. EFFECT OF LOAD POWER FACTOR AND PERCENTAGE OF THE CURRENT BALANCE

In order to analyze the effect of the total load power factor on the size of the voltage source, simulations are carried out between 70-80 kVA of load rating with a varying load power factor and varying load unbalance while nonlinear load is kept constant and the same is tabulated in Table VI. From the results, it is observed that the BESS is supplying more active power when the active power of the load increases due to better individual load power factors. At the same time, the reactive power fed by the voltage source decreases even after an increase in unbalance. Thus, there is a slight decrease in the kVA rating of the voltage source. Therefore, the effect of load Power factor on the sizing of a voltage source is also crucial.

The proposed analysis finally reveals that an uninterruptible power supply (UPS) with a 35-45% kVA size of that of the BESS and an overload capacity of 150-200%

can be chosen as the Voltage Source (VS) for the BESS. Thus, a judicious sizing of the UPS can be derived for the proposed microgrid system, which can serve critical loads and also act as VS/UPS for BESS during a utility grid outage. This method helps in avoiding oversizing VS and hence critical loads in the network are not more than 45% of overall microgrid capacity. Also, this method proves that any stand-alone BESS can be integrated seamlessly into the microgrid with DERs in a cost-effective manner by choosing the feasible sizing of the voltage source.

V. CONCLUSIONS

This work proposed a coordinated control of VS-BESS in a microgrid under two cases such as grid-connected and islanded mode. Comprehensive simulation and analytical studies were carried out using Matlab/Simulink with a chosen network configuration. The proposed model comprises of a detailed design of BESS and VS operated with hysteresis current control.

Considering the results and supporting discussion in previous section, it can be inferred that during outage of the grid, VS based BESS can supply both real and reactive power to the load. The proposed scheme shows great effectiveness for sizing the VS to drive the BESS against diverse loading conditions. The procedures for reference current generation for the BESS and active and reactive power-sharing between the VS and the BESS and percentage current unbalance calculation are also proposed. It was also seen that by providing proper time lapse between the events, ramping up of BESS is possible copiously. The effects of the percentage of load unbalance, nonlinear loads, and power factors are analyzed and the feasible sizing of VS ratings is computed for an effective hybrid microgrid.

Various load scenarios are discussed with a different combination of load current unbalance with various percentage of load nonlinearity to find out the optimum rating of VS for an efficient hybrid system design. This proposed method has laid a strong platform to find the most economic VS rating for given load patterns. It would be vital to further explore the effects of intermittent RES on sizing of the VS present on the microgrid network.

REFERENCES

- [1]. Mahmoud. Thair Shakir, et al. "The Role of Intelligent Generation Control Algorithms in Optimizing Battery Energy Storage Systems Size in Microgrids: A Case Study from Western Australia." *Energy Conversion and Management*, vol. 196, 2019, pp. 1335–52. Crossref, doi:10.1016/j.enconman.2019.06.045.
- [2]. Luo. Xing, et al. "Overview of Current Development in Electrical Energy Storage Technologies and the Application Potential in Power System Operation." *Applied Energy*, vol. 137, 2015, pp. 511–36. Crossref, doi:10.1016/j.apenergy.2014.09.081.

- [3]. Kucevic. Daniel, et al. "Standard Battery Energy Storage System Profiles: Analysis of Various Applications for Stationary Energy Storage Systems Using a Holistic Simulation Framework." *Journal of Energy Storage*, vol. 28, 2020, p. 101077. Crossref, doi:10.1016/j.est.2019.101077.
- [4]. Madurai. Elavarasan. Rajvikram, et al. "Investigations on Performance Enhancement Measures of the Bidirectional Converter in PV-Wind Interconnected Microgrid System." *Energies*, vol. 12, no. 14, 2019, p. 2672. Crossref, doi:10.3390/en12142672..
- [5]. Elavarasan. Rajvikram. Madurai., "The Motivation for Renewable Energy and Its Comparison with Other Energy Sources: A Review." *European Journal of Sustainable Development Research*, vol. 3, no. 1, 2019. Crossref, doi:10.20897/ejosdr/4005.
- [6]. Madurai. Elavarasan. Rajvikram., Leponraj Selvamanohar, et al. "A Holistic Review of the Present and Future Drivers of the Renewable Energy Mix in Maharashtra, State of India." *Sustainability*, vol. 12, no. 16, 2020, p. 6596. Crossref, doi:10.3390/su12166596.
- [7]. R. Krishnamoorthy et al. "An Assessment of Onshore and Offshore Wind Energy Potential in India Using Moth Flame Optimization." *Energies*, vol. 13, no. 12, 2020, p. 3063. Crossref, doi:10.3390/en13123063..
- [8]. Anthony. Mohanasundaram, et al. "Design of Rotor Blades for Vertical Axis Wind Turbine with Wind Flow Modifier for Low Wind Profile Areas." *Sustainability*, vol. 12, no. 19, 2020, p. 8050. Crossref, doi:10.3390/su12198050..
- [9]. Datta. Ujjwal, et al. "The Relevance of Large-Scale Battery Energy Storage (BES) Application in Providing Primary Frequency Control with Increased Wind Energy Penetration." *Journal of Energy Storage*, vol. 23, 2019, pp. 9–18. Crossref, doi:10.1016/j.est.2019.02.013.
- [10]. Dubarry. Matthieu, et al. "Battery Energy Storage System Battery Durability and Reliability under Electric Utility Grid Operations: Analysis of 3 Years of Real Usage." *Journal of Power Sources*, vol. 338, 2017, pp. 65–73. Crossref, doi:10.1016/j.jpowsour.2016.11.034.
- [11]. Killer. Marvin, et al. "Implementation of Large-Scale Li-Ion Battery Energy Storage Systems within the EMEA Region." *Applied Energy*, vol. 260, 2020, p. 114166. Crossref, doi:10.1016/j.apenergy.2019.114166.
- [12]. Baure. George and Matthieu Dubarry, "Battery Durability and Reliability under Electric Utility Grid Operations: 20-Year Forecast under Different Grid Applications." *Journal of Energy Storage*, vol. 29, 2020, p. 101391. Crossref, doi:10.1016/j.est.2020.101391.
- [13]. Hossain. Eklas, et al. "A Comprehensive Review on Energy Storage Systems: Types, Comparison, Current Scenario, Applications, Barriers, and Potential Solutions, Policies, and Future Prospects." *Energies*, vol. 13, no. 14, 2020, p. 3651. Crossref, doi:10.3390/en13143651.
- [14]. Hossain. Eklas et al. "Feasibility Analysis: Evaluating Sites for Possible Renewable Energy Options and Their Implications to Minimize the Cost." *The International Journal of Electrical Engineering & Education*, 2020, p. 002072092092853. Crossref, doi:10.1177/0020720920928537.
- [15]. Hadi. Abdullah Al et al. "Algorithm for Demand Response to Maximize the Penetration of Renewable Energy." *IEEE Access*, vol. 8, 2020, pp. 55279–88. Crossref, doi:10.1109/access.2020.2981877.
- [16]. Bila. M. et al. "Grid Connected Performance of a Household Lithium-Ion Battery Energy Storage System." *Journal of Energy Storage*, vol. 6, 2016, pp. 178–85. Crossref, doi:10.1016/j.est.2016.04.001.
- [17]. Opiyo. Nicholas, "Energy Storage Systems for PV-Based Communal Grids." *Journal of Energy Storage*, vol. 7, 2016, pp. 1–12. Crossref, doi:10.1016/j.est.2016.05.001.
- [18]. Pérez. G. and A. Conde, "Frequency Regulation of a Weak Microgrid through a Distribution Management System." *Electric Power Systems Research*, vol. 184, 2020, p. 106320. Crossref, doi:10.1016/j.epr.2020.106320.
- [19]. Sun. Qixing, et al. "Design and Test of a New Two-Stage Control Scheme for SMES-Battery Hybrid Energy Storage Systems for Microgrid Applications." *Applied Energy*, vol. 253, Elsevier BV, Nov. 2019, p. 113529. Crossref, doi:10.1016/j.apenergy.2019.113529.
- [20]. Christakou. Konstantina, "A Unified Control Strategy for Active Distribution Networks via Demand Response and Distributed Energy Storage Systems." *Sustainable Energy, Grids and Networks*, vol. 6, Elsevier BV, June 2016, pp. 1–6. Crossref, doi:10.1016/j.segan.2016.01.001.
- [21]. Zhong. Qing et al, "Optimal Siting & Sizing of Battery Energy Storage System in Active Distribution Network", *IEEE Transl. Innovative Smart Grid Technologies Europe*, October 2013.
- [22]. "Lithium-ion Battery Overview", Issue 10, May 2012. Available at: http://www.lightingglobal.org/wpcontent/uploads/bsk_pdf-manager/67_Issue10_Lithium_ionBattery_TechNote_final.pdf.
- [23]. Teleke. Sercan et al. "Rule-Based Control of Battery Energy Storage for Dispatching Intermittent Renewable Sources." *IEEE Transactions on Sustainable Energy*, vol. 1, no. 3, Institute of Electrical and Electronics Engineers (IEEE), Oct. 2010, pp. 117–24. Crossref, doi:10.1109/tste.2010.2061880.
- [24]. Matthew. T, et al. "Battery Energy Storage System (BESS) and Battery Management System (BMS) for Grid-Scale Applications", *Proceedings of the IEEE*, 10.1109/JPROC.2014.2317451
- [25]. Nayeem. A, et al. "Unbalanced Operation of Per-Phase Vector Controlled Four-Leg Grid Forming Inverter for Stand-Alone Hybrid Systems", 978-1-4673-2421-2012 IEEE.
- [26]. Ravinder. Singh et al. "Battery Energy Storage System for Power Conditioning", *National Power Systems Conference, NPSC 2004, Indian Institute of Technology, Madras DEC 27-30*.
- [27]. Kerdphol. Thongchart et al. "Optimal Sizing of Battery Energy Storage System in Microgrid System Considering Load Shedding Scheme." *International Journal of Smart Grid and Clean Energy*, 2014. Crossref, doi:10.12720/sgce.4.1.22-29.
- [28]. Bhim. Singh et al. "Application of Battery Energy Operated System to Isolated Power Distribution Systems", *PEDS*, 2007.
- [29]. Abusara. Mohammad A., et al. "Line-Interactive UPS for Microgrids." *IEEE Transactions on Industrial Electronics*, vol. 61, no. 3, Institute of Electrical and Electronics Engineers, Mar. 2014, pp. 1292–300. Crossref, doi:10.1109/tie.2013.2262763.
- [30]. Swaminathan. G., et al. "Investigations of Microgrid Stability and Optimum Power Sharing Using Robust Control of Grid Tie PV Inverter." *Lecture Notes in Electrical Engineering*, Springer Singapore, 2017, pp. 379–87. Crossref, doi:10.1007/978-981-10-4286-7_37.
- [31]. Christakou. Konstantina. "A Unified Control Strategy for Active Distribution Networks via Demand Response and

Distributed Energy Storage Systems.” *Sustainable Energy, Grids and Networks*, vol. 6, Elsevier BV, June 2016, pp. 1–6. *Crossref*, doi:10.1016/j.segan.2016.01.001.

- [32]. Zhong. Qing. et al. “Optimal Siting & Sizing of Battery Energy Storage System In Active Distribution Network”, *IEEE Transl. Innovative Smart Grid Technologies Europe*, October 2013



SWAMINATHAN GANESAN (M'17-SM'18) is currently with the Schneider Electric, Research and Development in renewable Energy division, India. Previously He worked in ABB corporate research center, India in Power System & Power Products division and worked in Power generation division in Alstom Power Conversion, India. He has more than 20 years of R&D experience. He has published several research articles in national and international journals and conferences. He has also coauthored book chapters and technical articles on Smart grid, Microgrid and integration of renewable energy and allied areas. He is a member of IEEE PES. He has been an Executive Member, from 2018 to 2020. His research interest includes Condition Monitoring, power electronics drives, Renewable energy and smart grid.



UMASHANKAR SUBRAMANIAM (M'11-SM'18) is currently with the Renewable Energy Lab, Department of Communications and Networks, College of Engineering, Prince Sultan University, Saudi Arabia. Previously He worked as an Associate Professor, the Head of the VIT Vellore, a Senior R&D, and a Senior Application Engineer in the field of power electronics, renewable energy, and electrical drives. He has more than 16 years of teaching, research, and industrial R&D experience. He has published more than 250 research articles in national and international journals and conferences. He has also authored/coauthored/contributed 20 books/chapters and 15 technical articles on power electronics applications in renewable energy and allied areas. He is a member of PES, PSES and YP. He was an Executive Member, from 2014 to 2016 and the Vice Chair of the IEEE MAS Young Professional, from 2017 to 2019. He received Danfoss Innovator Award-Mentor, from 2014 to 2015 and 2017 to 2018, the Research Award from VIT University, from 2013 to 2018. He held positions as the Vice Chair the IEEE Madras Section and the Chair the IEEE Student Activities, from 2018 to 2019. He is an Editor of *Heliyon*, Springer Nature and IEEE Access. He also received the INAE Summer Research Fellowship, in 2014. Under his guidance, 24 P.G. students and more than 25 U.G. Students completed the senior design project work. Also, six Ph.D. scholars completed Doctoral thesis as a Research Associate. He is also involved in collaborative research projects with various international and national level organizations and research institutions. His research interest includes power electronics, sustainability, energy and smart grid.



AJIT A. GHODKE (M'08-SM'16) received the B.E. degree in electrical engineering from Walchand College of Engineering, Sangli, Maharashtra, India, the M.E. degree in power systems from University of Pune, Maharashtra, India, and the Ph.D. degree from the Indian Institute of Technology Bombay in 2013. During 2006-2007, he was working as a Research Assistant with the Indian Institute of Technology Bombay, where he was involved with a project on development of scaled models for study of FACTS, HVDC and power system dynamics, which was sponsored by the Central Power Research Institute, Bangalore, India. Presently, he is working with Schneider Electric India, Bangalore as a Principal Technical Expert. His current research interests are microgrids, distributed generation, multilevel converters, and uninterruptible power supplies.



RAJVIKRAM MADURAI ELAVARASAN received the B.E. degree in electrical and electronics engineering from Anna University, Chennai, and the M.E. degree in power system engineering from the Thiagarajar College of Engineering, Madurai. He held an Associate Technical Operations position with IBM Global Technology Services Division. He was an Assistant Professor with the Department of Electrical and Electronics, Sri Venkateswara College of Engineering, Sriperumbudur, India.

His research interests include renewable energy and smart grid, wind energy research, power system operation and control, and artificial intelligence control techniques. He serves as a Recognised Reviewer for reputed journals, such as the IEEE *SYSTEMS JOURNAL*, *IEEE ACCESS*, *IEEE Communications Magazine*, the *International Transactions on Electrical Energy Systems* (Wiley), *Energy Sources, Part A: Recovery, Utilization and Environmental Effects* (Taylor and Francis), *Scientific Reports* (Springer Nature), *Chemical Engineering Journal* (Elsevier), *CFD Letters*, and *3 Biotech* (Springer).



KANNADASAN RAJU graduated from Vel Tech Engineering College, Chennai. He received his M.E. degree and Ph.D. from the College of Engineering Guindy, Anna University, Chennai, Tamil Nadu, India. Currently, he is working as an Assistant Professor in the Department of Electrical and Electronics Engineering, Sri Venkateswara College of Engineering, Sriperumbudur, Chennai, India. His area of interest is the design of metal oxide arresters for very fast transients, insulation coordination, synthesis of metal oxide nanoparticles, material processing, Flexible AC Transmission Systems, Smart waste management system and Electric Vehicles. He has published papers in international journals, international and national conferences. He is an Editorial member of American journal of electrical power and energy systems.



MAHAJAN SAGAR BHASKAR (Member, IEEE) received the bachelor's degree in electronics and telecommunication engineering from the University of Mumbai, Mumbai, India, in 2011 and the master's degree in power electronics and drives from VIT University, India, in 2014, and the Ph.D. degree in electrical and electronic engineering, University of Johannesburg, South Africa, in 2019. He worked as a Researcher Assistant with the Department of Electrical Engineering, Qatar University, Doha, Qatar, from 2018 to 2019. He worked

as a Research Student with the Power Quality Research Group, Department of Electrical Power Engineering, Universiti Tenaga Nasional (UNITEN), Private University, Kajang, Kuala Lumpur, Malaysia, from August 2017 to September 2017. He is currently with the Renewable Energy Lab, Department of Communications and Networks Engineering, College of Engineering, Prince Sultan University, Riyadh, Saudi Arabia. He has authored 100 plus scientific articles particular reference to X.Y. converter family, multilevel DC/DC and DC/AC converter, and high-gain converter. He received the Best Paper Research Paper Awards from the IEEE-CENCON'19, IEEE-ICCPCT'14, IET-CEAT'16, and ETAEERE'16 sponsored Lecture note in electrical engineering, (Springer). He is a member of the IEEE Industrial Electronics, Power Electronics, Industrial Application, and Power and Energy, Robotics and Automation, Vehicular Technology Societies, Young Professionals, various IEEE Councils and Technical Communities. He is a Reviewer Member of various international journals and conferences including IEEE and IET. He received the IEEE Access Award Reviewer of Month, in January 2019, for his valuable and thorough feedback on manuscripts, and for his quick turnaround on reviews.